Quantum teleportation in a solid-state system

John H. Reina* and Neil F. Johnson†
Physics Department, Clarendon Laboratory, Oxford University, Oxford, OX1 3PU, England
(Received 5 August 1999; published 8 December 2000)

We propose a practical solid-state system capable of demonstrating quantum teleportation. The setup exploits recent advances in the optical control of excitons in coupled quantum dots, in order to produce maximally entangled Bell and Greenberger-Horne-Zeilinger states. Only two unitary transformations are then required: a quantum controlled-*NOT* gate and a Hadamard gate. The laser pulses necessary to generate the maximally entangled states, and the corresponding unitary transformations, are given explicitly.

DOI: 10.1103/PhysRevA.63.012303 PACS number(s): 03.67.Lx, 03.65.Ta, 73.61.−r, 85.35.Be

Since the original idea of quantum teleportation considered in 1993 by Bennett *et al.* [1], great efforts have been made to realize the physical implementation of teleportation devices [2]. The general scheme of teleportation [1], which is based on Einstein-Podolsky-Rosen pairs [3] and Bell measurements [4] using classical and purely nonclassical correlations, enables the transportation of an arbitrary quantum state from one location to another without knowledge or movement of the state itself through space. This process has been explored from various points of view [2]; however none of the experimental setups to date have considered a solid-state approach, despite the recent advances in semiconductor nanostructure fabrication and measurement [5–8]. Reference [5], for example, demonstrates the remarkable degree of control that is now possible over quantum states of individual quantum dots (QDs) using ultrafast spectroscopy. The possibility therefore exists to use optically driven QDs as ''quantum memory'' elements in quantum computation operations, via a precise and controlled excitation of the system. In this paper, we propose a practical scheme for quantum teleportation that exploits currently available ultrafast spectroscopy techniques in order to prepare and manipulate entangled states of excitons in coupled QDs. To our knowledge, this is the first practical proposal for demonstrating quantum teleportation in a solid-state system.

In order to implement the quantum operations for the description of the teleportation scheme proposed here, we employ two elements: the quantum controlled-*NOT* gate and the Hadamard transformation. In the orthonormal computation basis of single qubits $\{|0\rangle,|1\rangle\}$, the controlled-*NOT* gate acts on two qubits $|\varphi_i\rangle$ and $|\varphi_j\rangle$ simultaneously as follows: $\mathcal{C}_{ij}(|\varphi_i\rangle|\varphi_j\rangle)\mapsto|\varphi_i\rangle|\varphi_i\oplus\varphi_j\rangle$. Here $\oplus$ denotes addition modulo 2. The indices i and j refer to the control bit and the target bit, respectively. The Hadamard transformation H acts only on single qubits by performing the rotations $H(|0\rangle)\mapsto(1/\sqrt{2})(|0\rangle+|1\rangle)$ and $H(|1\rangle)\mapsto(1/\sqrt{2})(|0\rangle-|1\rangle)$. We also introduce a pure state $|\Psi\rangle$ in this Hilbert space given by $|\Psi\rangle=\alpha|0\rangle+\beta|1\rangle$ with $|\alpha|^2+|\beta|^2=1$, where α and β are complex numbers. As discussed later, $|0\rangle$ represents the vacuum state for excitons while $|1\rangle$ represents a single exciton.

Figure 1 shows our general computational approach, which is inspired by the work of Brassard *et al.* [9]. As usual, we refer to two parties, Alice and Bob. Alice wants to teleport an arbitrary, unknown qubit state $|\Psi\rangle$ to Bob. Figure 2 shows the specific realization we are proposing using optically controlled quantum dots with QD *a* initially containing $|\Psi\rangle$. Alice prepares two qubits (QDs *b* and *c*) in the state $|0\rangle$ and then gives the state $|\Psi 00\rangle$ as the *input* to the system. By performing the series of transformations shown in Fig. 1(a), Bob receives as the *output* of the circuit the state $(1/\sqrt{2})(|0\rangle+|1\rangle)_a(1/\sqrt{2})(|0\rangle+|1\rangle)_b|\Psi\rangle_c$ [Fig. 2(d)]. In Fig. 1(b), we extend the analysis of the teleportation process to the case of a four-qubit quantum circuit, which can be realized by four coupled QDs. As before, Alice wants to teleport the state $|\Psi\rangle_a$ to Bob. She prepares three qubits in the state $|0\rangle$ (QDs *b*, *c*, and *d*) and gives the state $|\Psi 000\rangle$ as the input to the system. From Fig. 1(b), it is clear that the function of the first three operations performed by Alice is to obtain the maximally entangled Greenberger-Horne-Zeilinger (GHZ) state $(1/\sqrt{2})(|000\rangle+|111\rangle)$ [10]. The next two operations realized by Alice [before the dashed line in Fig. 1(b)] leave the system in the state

$$\tfrac{1}{2}\{|000\rangle(\alpha|0\rangle+\beta|1\rangle)+|011\rangle(\beta|0\rangle+\alpha|1\rangle)+|100\rangle(\alpha|0\rangle-\beta|1\rangle)+|111\rangle(-\beta|0\rangle+\alpha|1\rangle)\}. \quad (1)$$

Performing the operations shown after the dashed line in Fig. 1(b), Bob gets as the output of the circuit the state $(1/\sqrt{2})(|0\rangle+|1\rangle)_a(1/\sqrt{2})(|00\rangle+|11\rangle)_{b,c}|\Psi\rangle_d$. Hence the state $|\Psi\rangle$ was teleported from dot *a* to dot *d* in the system. In order to describe in detail how this circuit may be implemented, we need to perform the following steps: Alice prepares three qubits in the state $|0\rangle$, and then sends the first two of them through the two first gates between QDs *b* and *c*, as shown in Fig. 1(b). She keeps the information stored in QD *c*, namely, γ, in her quantum memory and sends qubit β to Bob. In the next step, she pushes the other qubit that is in state $|0\rangle$ together with γ to the third gate; after this operation, she keeps the last qubit of the system, δ. Alice then receives from QD *a* the qubit $|\Psi\rangle$ that she wants to teleport to Bob. To achieve this, she removes the δ qubit from her quantum memory and sends this, together with qubit $|\Psi\rangle$, to the next two gates of the circuit. She then performs a mea-

*Electronic address: j.reina-estupinan@physics.ox.ac.uk
†Electronic address: n.johnson@physics.ox.ac.uk

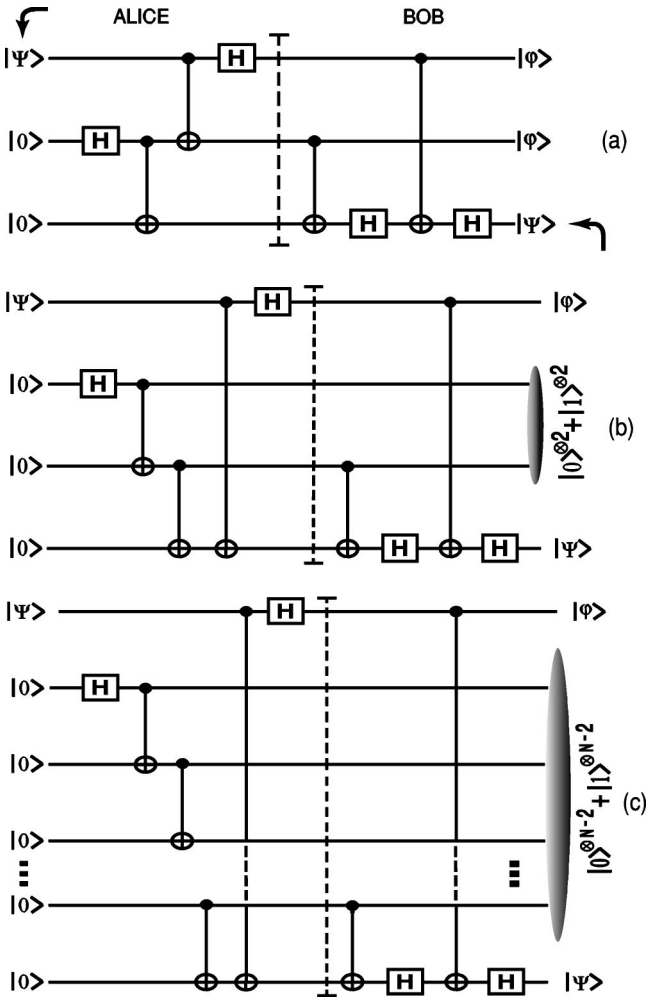

FIG. 1. Circuit schemes to teleport an unknown quantum state from Alice to Bob using an arrangement of (a) 3, (b) 4, and (c) n qubits (coupled quantum dots). The methods employ (a) Bell, (b) GHZ, and (c) Schrödinger's cat states, respectively.

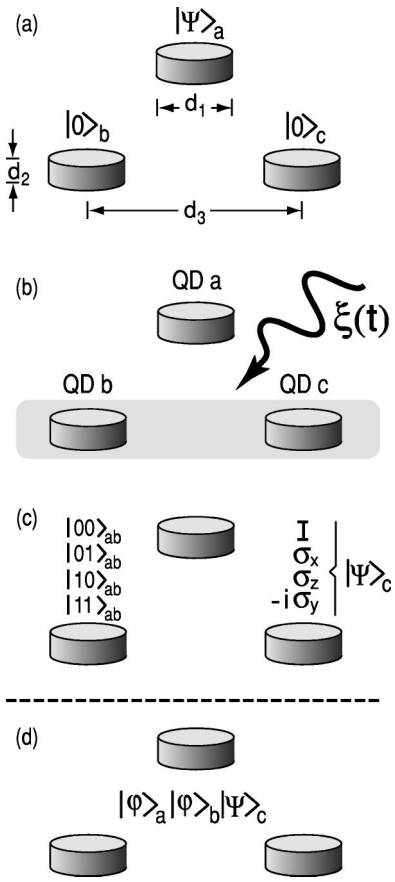

FIG. 2. Practical implementation of teleportation using optically driven coupled quantum dots. (a) Initial state of the system. (b) Intermediate step: radiating the system with the pulse $\xi(t)$. (c) Bell basis measurement and the quantum state of the system at the dashed line in Fig. 1(a). (d) Final state. Typical values for the dots are diameter $d_1=30$ nm, thickness $d_2=3$ nm and separation $d_3=50$ nm.

surement of the output between QDs a and c [11] [at the dashed line in Fig. 1(b)] in order to turn the result into two classical bits Λ and Γ, respectively. To finish the teleportation process, Alice needs to communicate Λ and Γ to Bob via a classical communication channel. Hence after the dashed line, Bob receives the classical information and creates the quantum states $|\Lambda\rangle$ and $|\Gamma\rangle$. Next, he removes the qubits β and δ from his quantum memory and sends the four qubits to his part of the circuit. At this point teleportation is complete since Bob receives at his output the state $|\Psi\rangle$ on dot d. Hence our quantum teleportation circuit (QTC) transforms the input $|\Psi\rangle_a|0\rangle_b|0\rangle_c|0\rangle_d$ into the output $(1/\sqrt{2})(|0\rangle+|1\rangle)_a|Bell\rangle_{b,c}|\Psi\rangle_d$.

Interestingly, the above teleportation process can be extended to an n QTC using the Schrödinger's cat state, as shown in Fig. 1(c). Again, the goal is to teleport the state $|\Psi\rangle_{a_1}$ from Alice to Bob. She prepares $n-1$ qubits in the state $|0\rangle$ (QDs $a_2,a_3,\ldots,a_n$) and hence gives the state $|\Psi 00\ldots0\rangle$ as the input. After the first $n-1$ operations [Fig. 1(c)] she obtains, between dots $a_2,a_3,\ldots a_n$, the Schrödinger's cat state $(1/\sqrt{2})(|00\ldots0\rangle+|11\ldots1\rangle)_{a_2,\ldots a_n}$ which, followed by the last two exclusive-OR operations before the dashed line, leaves the system in the following state of n qubits:

$$\tfrac{1}{2}\{|00\ldots0\rangle(\alpha|0\rangle+\beta|1\rangle)+|011\ldots1\rangle(\beta|0\rangle+\alpha|1\rangle) +|100\ldots0\rangle(\alpha|0\rangle-\beta|1\rangle) +|11\ldots1\rangle(-\beta|0\rangle+\alpha|1\rangle)\}. \quad (2)$$

The procedure to realize the circuit of Fig. 1(c) follows directly from the description given for Fig. 1(b). In the case of Fig. 1(c), the measurement performed by Alice at the end of her part of the circuit must be realized between the a_1th and the a_{n-1}th QDs [11] in order to turn the result into two classical bits Θ and Υ, respectively. Hence Alice communicates these bits to Bob via a classical channel and, after the dashed line, Bob receives the classical information and creates the quantum states $|\Theta\rangle$ and $|\Upsilon\rangle$. Next, he removes from his quantum memory the other $n-2$ qubits, thereby ultimately obtaining $|\Psi\rangle$ on the nth dot. In this way, the QTC presented here transforms the input state

$|\Psi\rangle_{a_1}|0\rangle_{a_2}|0\rangle_{a_3}\ldots|0\rangle_{a_n}$ into the output $(1/\sqrt{2})(|0\rangle + |1\rangle)_{a_1}(1/\sqrt{2})(|00\ldots0\rangle + |11\ldots1\rangle)_{a_2,\ldots,a_{n-1}}|\Psi\rangle_{a_n}$. From Figs. 1(b) and 1(c) we note that the final stage of the QTC may be used as a subroutine in larger quantum computations or for quantum communication; specifically this is because we are recovering at the output a 2,3, . . . , or $(n-2)$-*maximally* entangled state [12]. We also note that the structure of Bob's part of the circuit is the same for all the circuits in Fig. 1. This is because Bob's function in the QTC is to realize the ''appropriate rotations'' over the general state given in Eq. (2). It is interesting to note that if Bob, instead of performing the operations after the dashed line, chooses one of these appropriate unitary transformations [13] to apply to the nth qubit after receiving the classical bits from Alice's measurement (subindices of U in Ref. [13]), then he does not need to perform his part of the circuit, since this transformation leaves dot a_n in the state $|\Psi\rangle$. For this reason only two unitary exclusive-*OR* transformations are needed in order to teleport the state $|\Psi\rangle$. However, from the point of view of our implementation and, more generally, for quantum computer algorithms, it is better to undertake the complete process shown in the QTC than to choose such a special rotation. Although our goal is the practical realization using what is at the limit of current optoelectronics technology, we note that the circuits of Fig. 1 *are not restricted* to QD systems: they can be applied to any system where the task of entangled-state preparation has been achieved.

In order to describe the physical implementation of the quantum circuits using coupled quantum dots, we exploit the recent experimental results involving coherent control of excitons in single quantum dots on the nanometer and femtosecond scales [5,6]. Consider a system of N identical and equispaced QDs containing no net charge that are radiated by long-wavelength classical light, as illustrated schematically in Fig. 2(b) for the case $N=3$. In the frame of the *rotating wave approximation*, the formation of single excitons within the individual QDs and their interdot hopping are described by the Hamiltonian ($\hbar=1$)[14,15]

$$H=\Delta_\omega J_2+A(J_+ + J_-)+W(J^2-J_z^2), \tag{3}$$

where

$$J_+=\sum_{p=1}^{N} c_p^\dagger h_p^\dagger,\quad J_-=\sum_{p=1}^{N} h_p c_p,$$

$$J_z=\tfrac{1}{2}\sum_{p=1}^{N}\{c_p^\dagger c_p - h_p h_p^\dagger\}. \tag{4}$$

Here, $c_p^\dagger$ ($h_p^\dagger$) is the electron (hole) creation operator in the pth QD; $\Delta_\omega=\epsilon-\omega$ is the detuning parameter, ϵ represents the band gap, W is the interdot interaction parameter (Förster process), and $\xi(t)=A\exp(-i\omega t)$ is a radiation pulse of amplitude A (incident electric field strength) and central frequency ω. The quasispin J operators satisfy the usual commutation relations $[J_z,J_\pm]=\pm J_\pm$, $[J_+,J_-]=2J_z$, and $[J^2,J_+]=[J^2,J_-]=[J^2,J_z]=0$.

By solving the eigenvalue problem associated with the Hamiltonian (3), we have shown [14] for several different values of the phase ϕ, that Bell and GHZ states of the form

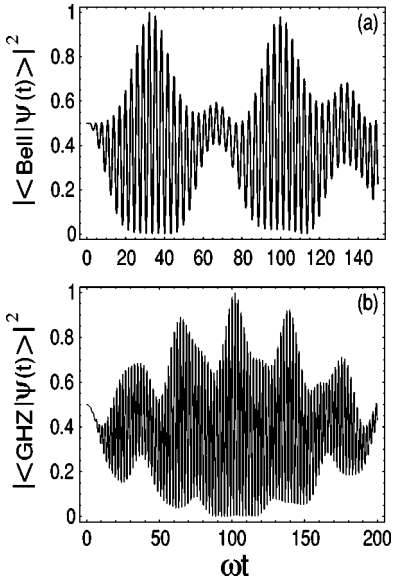

FIG. 3. Generation of (a) the Bell State $(1/\sqrt{2})(|00\rangle+|11\rangle)$, and (b) the GHZ state $(1/\sqrt{2})(|000\rangle+|111\rangle)$. These pulses correspond to the realization of the Hadamard gate followed by one controlled-*NOT* gate and two controlled-*NOT* gates, respectively [see Figs. 1(a) and 1(b)]. In units of the band gap $\epsilon=2.8$ eV, $W=0.1$, $A=1/25$. $|\psi(0)\rangle=|0\rangle$. Here, $\psi(t)$ denotes the total wave function of the system in the laboratory frame at time t.

$(1/\sqrt{2})(|00\rangle+e^{i\phi}|11\rangle)$ and $(1/\sqrt{2})(|000\rangle+e^{i\phi}|111\rangle)$ can be prepared in systems comprising two and three coupled quantum dots, respectively. The practical requirements are realizable in present experiments employing both ultrafast [5,6] and near-field optical spectroscopy [7] of quantum dots. In Fig. 3, we present the generation of ϕ pulses that lead to the implementation of our QTC. As mentioned previously, $|0\rangle$ represents the vacuum for excitons while $|1\rangle$ denotes a single-exciton state.

For the practical proposal of Fig. 1(a), we require three equidistant QDs that initially must be prepared in the state $|\Psi\rangle_a|0\rangle_b|0\rangle_c$. As shown in Fig. 2(a), one of these (QD a) contains the quantum state $|\Psi\rangle_a$ that we wish to teleport, while the other two (QDs b and c) are initialized in the state $|00\rangle_{bc}$—this latter state is easy to achieve since it is the ground state. Following this initialization, we illuminate QDs b and c with the radiation pulse $\xi(t)$ [see Fig. 2(b)]. As an example we consider the case of ZnSe-based QDs. The band gap $\epsilon=2.8$ eV, hence the resonance optical frequency $\omega=4.3\times10^{15}\ \text{s}^{-1}$. In units of ϵ, $W=0.1$ and $A=1/25$. For a 0 or 2π pulse, the density of probability for finding the QDs b and c in the Bell state $(1/\sqrt{2})(|00\rangle+|11\rangle)$ shows that a time $\tau_{Bell}=7.7\times10^{-15}$ s is required [see Fig. 3(a)]. This time τ_{Bell} hence corresponds to the realization of the first two gates of the circuit in Fig. 1(a), i.e., the Hadamard transformation (or $\pi/4$ rotation) over QD b followed by the controlled-*NOT* gate between QDs b and c. After this, the information in qubit c is sent to Bob and Alice keeps in her memory the state of QD b [Fig. 1(a)]. Next, we need to perform a controlled-*NOT* operation between QDs a and b and, following that, a Hadamard transform over the QD a: this procedure then leaves the system in the state

$$\tfrac{1}{2}\{|00\rangle(\alpha|0\rangle+\beta|1\rangle)+|01\rangle(\beta|0\rangle+\alpha|1\rangle)$$
$$+|10\rangle(\alpha|0\rangle-\beta|1\rangle)+|11\rangle(-\beta|0\rangle+\alpha|1\rangle)\}. \quad (5)$$

As it can be seen from Eq. (5), we are proposing the realization of the Bell basis measurement in two steps [9]: first, we have rotated from the Bell basis into the computational basis ($|00\rangle$, $|01\rangle$, $|10\rangle$, $|11\rangle$), by performing the unitary operations shown before the dashed line in Fig. 1(a). Hence, the second step is to perform a measurement in this computational basis. At this point, we leave QDs *a* and *b* in one of the four states $|00\rangle$, $|01\rangle$, $|10\rangle$, or $|11\rangle$ [see Fig. 2(c)], which are the four possible measurement results. This last step can be experimentally realized by using *near-field optical spectroscopy* [7]. In this way, it is possible to scan, dot by dot, the optical properties of the entire dot ensemble, and particularly, to measure directly the excitonic photoluminiscence spectrum of dots *a* and *b*, thus completing the Bell basis measurement. The result of this measurement provides us with two classical bits of information, conditional on the states measured by nanoprobing on QDs *a* and *b* [see Fig. 2(c)]. These classical bits are essential for completing the teleportation process: rewriting Eq. (5) as

$$\tfrac{1}{2}\{|00\rangle|\Psi\rangle+|01\rangle\sigma_x|\Psi\rangle+|10\rangle\sigma_z|\Psi\rangle+|11\rangle(-i\sigma_y)|\Psi\rangle\}, \quad (6)$$

we see that if instead of performing the set of operations shown after the dashed line in Fig. 1(a), Bob performs one of the conditional unitary operations I,σ_x,σ_z, or $-i\sigma_y$ [13] over the QD *c* [depending on the measurement results or classical signal communicated from Alice to Bob, as shown in Fig. 2(c)] the teleportation process is finished since the excitonic state $|\Psi\rangle$ has been teleported from dot *a* to dot *c*. This final step can be verified by measuring directly the excitonic luminescence from dot *c*, which must correspond to the initial state of dot *a*.

For instance, if the state to be teleported is $|\Psi\rangle\equiv|1\rangle$, the final measurement of the near-field luminiscence spectrum of dot *c* must give an excitonic emission line of the same wavelength and intensity as the initial one for dot *a*. This measurement method, used for verifying the fidelity of the process, can be used if we either perform the unitary transformations after Alice's measurement [Fig. 2(c)] or we realize the complete teleportation circuit shown in Fig. 1(a), leaving the system in the state shown in Fig. 2(d). Combining spatial and spectral resolutions, it has already been demonstrated that it is possible to excite and probe just one individual QD with the corresponding dephasing time $\tau_d=4\times10^{-11}$ s [5]. Hence we have the possibility of coherent optical control of the quantum state of a single dot. Furthermore, this mechanism can be extended to include more than one excited state: since $\tau_{Bell}/\tau_d\simeq1.8\times10^{-4}$, several thousand unitary operations can in principle be performed in this system before the excited state of the QD decoheres. This fact together with the experimental feasibility of applying the required sequence of laser pulses on the femtosecond time scale [17] leads us to conclude that we do not need to worry unduly about decoherence occurring while performing the unitary operations that Bob needs in order to obtain the final states schematically sketched in Figs. 2(c) and 2(d), thereby completing the teleportation process. In the case of Fig. 3(b), a similar analysis shows that $\tau_{GHZ}=1.3\times10^{-14}$ s, and hence $\tau_{GHZ}/\tau_d\simeq3.3\times10^{-4}$: this also makes the circuit in Fig. 1(b) experimentally feasible. Although this discussion refers to ZnSe-based QDs, other regions of parameter space can be explored by employing semiconductors of different band gap ϵ. We believe that hybrid organic-inorganic nanostructures [18] are very promising candidates for the setup proposed here. This is because these hybrid structures provide us with large radius (Wannier-Mott) exciton states in the inorganic material and small-radius (Frenkel) exciton states in the organic one [19]. Hence the hybrid material will be characterized by a radius dominated by their Wannier component and by an oscillator strength dominated by their Frenkel component. This means that the desirable properties of both the organic and the inorganic material are brought together to overcome basic limitations that arise if each one acts separately. Following recent results [18], if the 3 QD setup required in the present proposal is made of an inorganic II-VI material (e.g., the extensively studied ZnSe or ZnCdSe), embedded in bulklike organic crystalline material (e.g., tetracene, perylene, fullerene, PTCDA) where their Frenkel and Wannier excitons are in resonance with each other, we would expect a strong hybridization between these excitons, which means a greater Wannier exciton delocalization or Förster hopping. To achieve this, the typical distance between QDs should be of the same order as their size: In ZnSe, the Bohr radius of the three-dimensional Wannier exciton $a_B\approx35$ A, hence QDs with radii of about 50 A will considerably increase the binding energy of these excitons. If these dots are placed in an organic matrix (as discussed above) separated by a distance of the same order, we should be able to perform the appropriate quantum operations required in the teleportation process of the excitonic state $|\Psi\rangle$. A more detailed description of the implementation of the quantum entanglement schemes required in the present proposal is given in Ref. [14]. Even though the structures that we are considering have a dephasing time of order 10^{-11} s, QDs with stronger confinement are expected to have even smaller coupling to phonons giving the possibility of much longer intrinsic coherence times.

In summary, we have proposed a practical implementation of a quantum teleportation device, exploiting current levels of optical control in coupled QDs. Furthermore, the analysis suggests that several thousand quantum computation operations may in principle be performed before decoherence takes place.

The authors thank L. Quiroga, J. Erland, D.J.T. Leonard, and S.C. Benjamin for helpful discussions. J.H.R. thanks the financial support of COLCIENCIAS and gratefully acknowledges H. Steers for continuous encouragements.

[1] C.H. Bennett, G. Brassard, C. Crépeau, R. Jozsa, A. Peres, and W.K. Wooters, Phys. Rev. Lett. **70**, 1895 (1993).

[2] D. Bowmeester, J.W. Pan, K. Mattle, M. Eibl, H. Weinfurter, and A. Zeilinger, Nature (London) **390**, 575 (1997); D. Boschi, S. Branca, F. De Martini, L. Hardy, and S. Popescu, Phys. Rev. Lett. **80**, 1121 (1998); A. Furusawa, J.L. Sorensen, S.L. Braunstein, C.A. Fuchs, H.J. Kimble, and E.S. Polzik, Science **282**, 706 (1998); M.A. Nielsen, E. Knill, and R. Laflamme, Nature (London) **396**, 52 (1998).

[3] A. Einstein, B. Podolsky, and N. Rosen, Phys. Rev. **47**, 777 (1935).

[4] S.L. Braunstein, A. Mann, and M. Revzen, Phys. Rev. Lett. **68**, 3259 (1992).

[5] N.H. Bonadeo, J. Erland, D. Gammon, D.S. Katzer, D. Park, and D.G. Steel, Science **282**, 1473 (1998).

[6] N.H. Bonadeo, G. Chen, D. Gammon, D.S. Katzer, D. Park, and D.G. Steel, Phys. Rev. Lett. **81**, 2759 (1998).

[7] A. Chavez-Pirson, J. Temmyo, H. Kamada, H. Gotoh, and H. Ando, Appl. Phys. Lett. **72**, 3494 (1998).

[8] N.F. Johnson, J. Phys.: Condens. Matter **7**, 965 (1995).

[9] G. Brassard, S.L. Braunstein, and R. Cleve, Physica D **120**, 43 (1998).

[10] D.M. Greenberger, M.A. Horne, A. Shimony, and A. Zeilinger, Am. J. Phys. **58**, 1131 (1990).

[11] Since the first and third qubits are working in Bob's part of the circuit only as the control bit of the controlled-*NOT* gates, this procedure can be performed without affecting the final outcome of the computation (see also Ref. [16]). The same is true for the n-qubit circuit presented here, where the measurement is performed between the first and the $(n-1)$th qubits.

[12] In the case of an m-qubit circuit as presented here, the output is a state that contains the $(m-2)$-*maximally* entangled state $(1/\sqrt{2})(|00\ldots0\rangle+|11\ldots1\rangle)_{2,3,\ldots,m-1}$.

[13] These unitary transformations, which depend on the result of Alice's measurement (subindices of U), are the Pauli matrices

$$U_{00}\equiv I=\begin{pmatrix}1 & 0\\ 0 & 1\end{pmatrix},\quad U_{01}\equiv\sigma_x=\begin{pmatrix}0 & 1\\ 1 & 0\end{pmatrix},$$

$$U_{10}\equiv\sigma_z=\begin{pmatrix}-1 & 0\\ 0 & 1\end{pmatrix},\quad U_{11}\equiv-i\sigma_y=\begin{pmatrix}0 & -1\\ 1 & 0\end{pmatrix}.$$

[14] J.H. Reina, L. Quiroga, and N.F. Johnson, Phys. Rev. A **62**, 012305 (2000).

[15] L. Quiroga and N.F. Johnson, Phys. Rev. Lett. **83**, 2270 (1999).

[16] R.B. Griffiths and C.-S. Niu, Phys. Rev. Lett. **76**, 17 (1996).

[17] J. Erland (private communication).

[18] See, e.g., V.M. Agranovich, D.M. Basko, G.C. La Rocca, and F. Bassani, J. Phys. Condens. Matter **10**, 9369 (1998); Phys. Status Solidi A **178**, 69 (2000).

[19] There are two models conventionally used to classify excitons: the small-radius Frenkel exciton model and the large-radius Wannier-Mott exciton model. Frenkel excitons in organic crystals have radii comparable to the lattice constant $a\approx5$A. Wannier excitons in semiconductor quantum wells have large Bohr radii: $a_B\approx100$A in III-V materials (e.g., GaAlAs) and $a_B\approx30$A in II-VI ones (e.g., ZnSe).